1. Experimental

Materials

Lithium bis(trifluoromethane)sulfonimide (LiTFSI) and 1,4-dioxane (DX) were purchased from Sigma-Aldrich. Lithium bis(fluorosulfonyl)imide (LiFSI) was provided by Chunbo Co., Ltd. The standard carbonate electrolyte containing 1.0 M lithium hexafluorophosphate ($LiPF_6$) in ethylene carbonate (EC): ethyl methyl carbonate (EMC): dimethyl carbonate (DMC) (1:1:1 by volume) was ordered from PANAX ETEC Co., Ltd. The lithium salts and solvents were all battery-grade. All the chemicals were stored and handled in an argon-filled glove box (<0.1 ppm H_2O and <0.1 ppm O_2). The formula of the standard electrolyte and low concentration electrolytes are as follows:

Standard electrolyte (STD): 1.0 M LiPF6 in EC:EMC:DMC (1:1:1 by volume)

Low concentration single-salt electrolyte (LSE): 0.5 M LiFSI in DX

Low concentration bisalt electrolyte (LBE): 0.3 M LiFSI + 0.2 M LiTFSI in DX

The lithium (Li) foil with a thickness of 250 μm was purchased from MTI corporation. The Celgard (polypropylene, 2400) separator, copper (Cu) foil, and aluminum (Al) foil were ordered from Wellcos corporation. The $LiFePO_4$ (LFP, MTI Corporation) cathode was prepared by mixing LFP, super P (Alfa Aesar), and poly(vinylidene difluoride (PVDF, Sigma Aldrich) (weight ratio = 8:1:1) and blading on an Al foil. Then, the electrodes were dried at 80 °C for 12 h, pressed, and punched into 15 mm disks. The LFP disks were further dried at 80 °C under vacuum for 24 h. All electrodes were kept in an Ar-filled glove box before the coin cells were made.

Measurement of physical properties

Ionic conductivity measurements were performed using a conductivity bench meter (S30, Mettler Toledo) and a Cond Probe Inlab710 (Mettler Toledo). The system was calibrated before each measurement using an aqueous 0.1 m KCl solution. Shear viscosity measurements were conducted using a Brookfield

rheometer DV3T. The viscometer was calibrated with deionized water. All the measurements were performed at 25 °C.

A contact angle tester (Ossila L2004A1) was used to take the pictures of the contact angles between the PP separator and the standard electrolyte, the low concentration single-salt electrolyte, and low concentration bisalt electrolyte.

Characterization of Solvation Structure

Laser Raman spectroscopy was performed at room temperature using a RamanTouch system (Nanophoton) with a laser wavelength of 532 nm. During the measurements, the samples were sealed in a capillary tube. The spectra were deconvoluted using a Gaussian–Lorentzian function spectroscopic analysis.

Coin-cell assembly

A Li||Cu cell was assembled by stacking Cu foil (19 mm in diameter), a PP separator, Li metal foil (15.6 mm in diameter) in a 2032 coin cell. A Li||Li symmetrical cell was assembled using the same method but replacing the Cu foil with Li foil. A Li||LFP cell was assembled by using an LFP cathode (15 mm in diameter with mass loading of 5.83 mg cm^{-2}) and Li foil. The 70 µL electrolyte was added to each cell. All the cells were assembled in an argon glove box.

Electrochemical Measurements

The conductivity of the wet separator was measured by using the stainless steel (SS)|wet separator|SS symmetric cell and calculated by the following equation:

$$\sigma_s = \frac{d}{A \times R_s} \qquad \text{(S1)}$$

where σ_s is the conductivity of the wet separator, d and A are corresponding to the thickness and contact area of the separator, respectively. R_s is the impedance of the SS|wet separator|SS symmetric cells, which can be obtained from the intercept of the Nyquist plot and x-axis.

The MacMullin number was determined by the following equation:

$$\text{MacMullin number} = \frac{\sigma_e}{\sigma_S} \qquad \text{(S2)}$$

where σ_e and σ_s represented the conductivity of the electrolyte and wet separator, respectively.

The lithium transference number (t_{Li+}) was measured using a combination of direct-current (DC) polarization and AC impedance in a symmetrical lithium cell. t_{Li+} can be calculated using following equation:

$$t_+ = \frac{I_{ss}\left(\Delta V - I_0 R_0\right)}{I_0\left(\Delta V - I_{ss} R_{ss}\right)} \qquad \text{(S3)}$$

where ΔV is the applied voltage (10 mV), and I_0 and I_{ss} are the initial currents and steady current, respectively, in the DC polarization process. R_0 and R_{ss} are the initial charge-transfer resistance and steady charge-transfer resistance, respectively, during the DC polarization process.

Linear sweep voltammetry (LSV) was performed to determine the electrochemical stability windows of the investigated electrolytes. A three-electrode cell system was employed with a platinum (Pt) disk as the working electrode and Li metal as both the counter and reference electrodes. LSV measurements were performed at a scan rate of 2 mV s^{-1}. Electrochemical impedance spectroscopy (EIS) in the frequency range of 10 mHz to 1.0 MHz with an amplitude of 10 mV was used to evaluate the electrolyte stability and resistance of the cell systems. The Li||Li symmetric cells were measured by EIS after 10, 24, and 48 h. Transference number, LSV, and EIS measurements were performed using a Bio-logic VMP3 instrument at 25 °C.

Galvanostatic experiments were carried out using CR2032-type coin cells on a WBCS3000L battery cycler system (Wonatech, Korea) at a constant temperature of 25 °C. The CE of the lithium electrode was examined using Li||Cu cells. The CE of coin cells was determined by the modified Method 3 reported by Adam et al.[1] To precondition the Cu substrate, a given amount of Li (4 mAh cm^{-2}) was first deposited on

the Cu foil at 0.4 mA cm^{-2} and subsequently stripped until the voltage reached 1.0 V *vs* Li/ Li^+. Then, a certain portion of charge (Q_T) is used to deposit Li onto the Cu substrate as a Li reservoir at 0.4 mA cm^{-2} for 10 h. For the next step, a smaller charge (Q_c) is used to cycle Li between two electrodes for 10 cycles. The final stripping charge (Q_S) of the remaining Li reservoir is determined with the cut-off voltage (1.0 V *vs.* Li/Li^+). The average CE was calculated by the formula described below:

$$CE_{avg} = \frac{10Q_C + Q_S}{10Q_C + Q_T} \qquad \text{(S4)}$$

The Li||LFP coin cells were monitored in galvanostatic mode within a voltage range of 2.5–4.0 V versus Li/Li^+. The Li||LFP cells were first cycled at 0.1 C for two cycles and then cycled at 0.5 C/1.0 C for charge/discharge process (1.0 C ≈ 170 mA g^{-1} based on LFP cathode materials).

Characterization of Electrodes

The morphology and surface components were investigated by scanning electron microscopy (SEM) and X-ray photoelectron spectroscopy (XPS). Before analysis, Li anode and LFP cathode were collected from Li||LFP cells and immersed in pure DME or DX solvent for 24 h. Afterward, the electrodes were washed several times by pure DME and DX to remove the salt residue and dried in the vacuum chamber of an Ar-filled glove box for 24 h. SEM images were taken using a Hitachi S4800 instrument at an accelerating voltage of 5 kV and an absorbed current of 10 μA. XPS measurements were conducted to characterize the chemical species using a K-alpha X-ray photoelectron spectrometer (Thermo Fisher) with a monochromatic Al Kα source (1,486.7 eV) for excitation. All spectra were referenced using the C 1s line at 285.0 V for comparison. All samples were prepared in a glove box and transported to SEM and XPS instruments in a glass container filled with Ar gas.

2. Computational Methods

Quantum mechanical calculations

Quantum mechanical calculations were performed using the Gaussian 09 program at the B3LYP/6-311++G(d,p) level.[2] The effects of solvation were considered with the integral equation formalism variant of the Conductor-like polarizable continuum model (CPCM). The binding energy (E_b) between two components was defined as follows:

$$E_b = E_{total} - E_A - E_B \qquad (S5)$$

where E_{total}, E_A, and E_B are the total energy of the A–B complexes, A component, and B component, respectively. A and B can be Li-ion, anions (FSI^- or $TFSI^-$), and solvents. The relative binding energies were determined using the equation below:

$$\text{Relative binding energy} = E_{Li^+ \text{ --- DX}} - E_{Li^+ \text{ --- anion}} \qquad (S6)$$

where $E_{Li^+ \text{ --- DX}}$ and $E_{Li^+ \text{ --- anion}}$ are the total energy of the Li^+---DX and Li^+---anion complexes, respectively.

Classical molecular dynamics

Classical molecular dynamics (CMD) simulations were conducted for the LSE and LBE electrolyte systems, using the LAMMPS software.[3] Table S3 summarizes the number of molecules simulated for each system. The force field parameters for Li^+ were obtained from Dang et al.,[4] while for FSI^- and $TFSI^-$ (except partial charges), the force paremeters from Pádua et al. were employed.[5] The partial charges for $TFSI^-$ were obtained from quantum calculations using the Gaussian 16 program,[2] where the structure for $TFSI^-$ was first optimized at the MP2/aug-cc-pvtz level of theory, followed by calculations of the electrostatic potential with the HF/6-31G(d) level of theory. The partial charges for $TFSI^-$ were then obtained from the RESP method availible in the AMBER software.[6] For DX, the OPLS force field was employed.[7] The partial charges for all ions were scaled to 0.7 times that of their original values, in order to mimic atomic polarizability.

All CMD simulations were performed with the NPT ensemble at 298K and 1 atm. The simulation box was first equilibriated for 10 ns. This was then followed by 20 ns production runs. The Nosé-Hoover thermostat and barostat with a time constant of 0.1 and 1 ps was used, respectively. The Particle–Particle Particle–Mesh method was used to determine long-range electrostatics interaction and a cutoff of 12.0 Å was used for nonbonded interactions. A time step of 1 fs was employed and the coordinates were saved every 0.1 ps for further analysis.The ionic conductivity (λ) can be calculated using the following Einstein relationship:[8]

$$\lambda = \lim_{t\to\infty} \frac{e^2}{6tVk_BT} \sum_{i,j}^{N} z_i z_j \left\langle \left[R_i(t) - R_i(0)\right] \times \left[(R_j(t) - R_j(0)\right] \right\rangle \qquad \text{(S7)}$$

where e is the electron charge, V is the volume of the simulation box, k_B is the Boltzmann's constant, T is the temperature, t is the time, z_i and z_j are the charges on ions i and j, respectively, and $R_i(t)$ and $R_j(t)$ are the displacements of ions i and i at time t, respectively. The summation is performed over all the ions. From the calculated densities and ionic conductivities in Table S4, it can be observed that the CMD simulations resasonbly reproduce experimetal trends. Hence, the choice of the force field used herein can sufficiently model the simulated systems.

Radial distrubution functions (RDFs) between Li^+ and the oxygen atoms of anion/solvent molecules were calculated to investigate the solvation structures present in the LSE and LBE electrolytes (Figure 1c-d). In order to characterize the type of solvation structures present in LSE/LBE, the coordination distribution of cations around the anions was determined (Figure 1b). The distance criteria for the inclusion of a cation around the anion was obtained from the first minima of the center-of-mass RDFs between the anion and the cation.

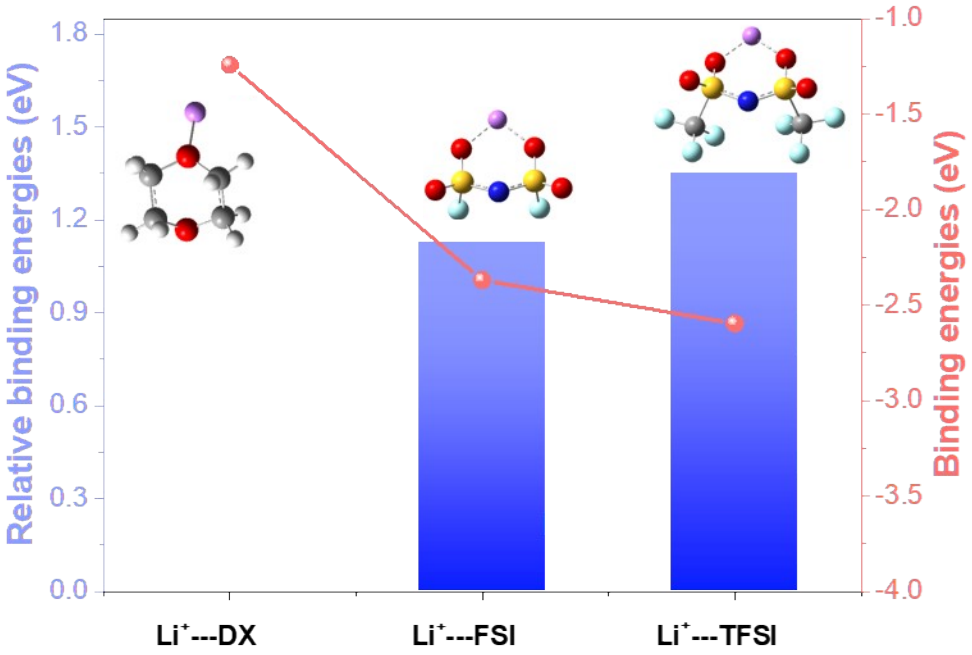

Figure S1. The binding energies between Li^+ and solvents/anions were obtained by calculations. Colors: oxygen, red; hydro, light gray; carbon, gray; lithium, purple; sulfur, yellow; nitrogen, blue; and fluorine, light cyan.

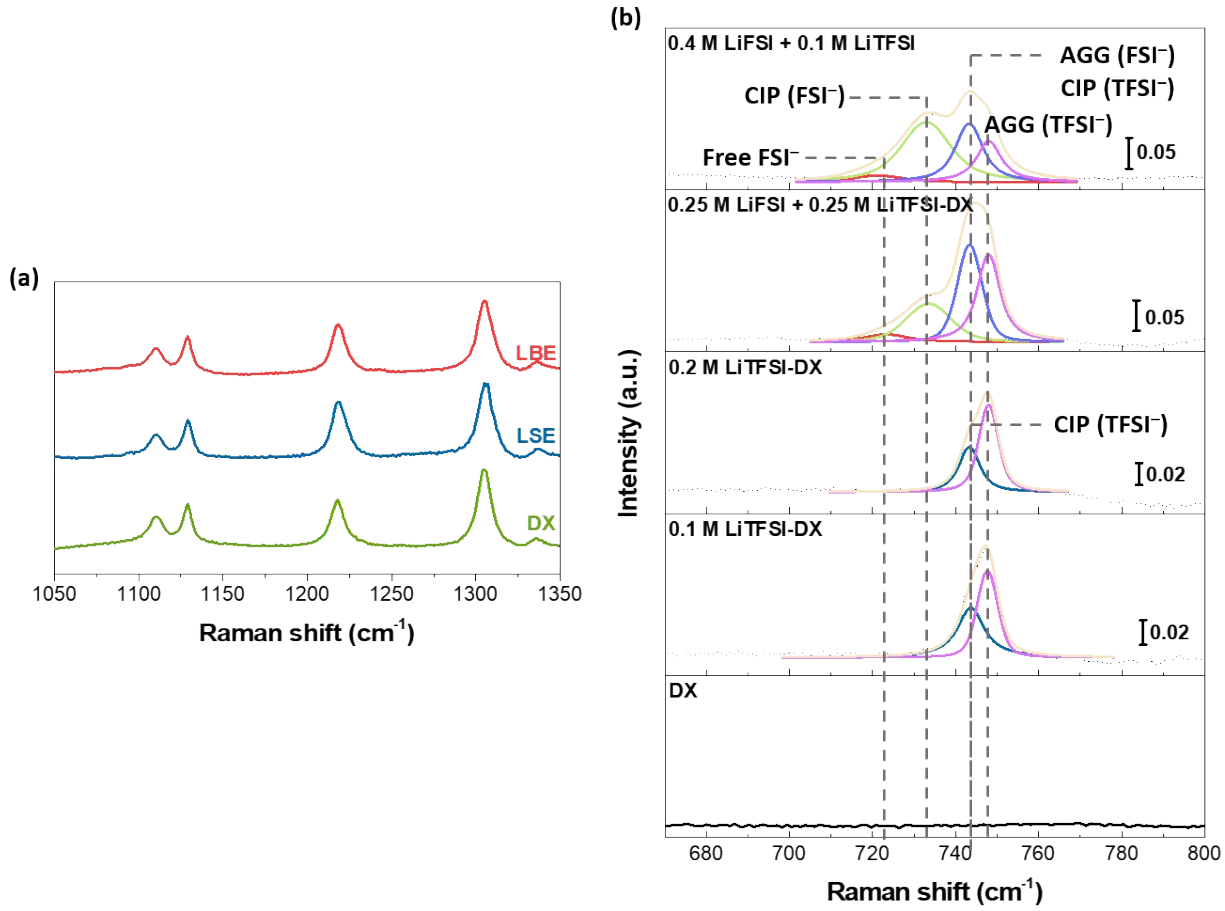

Figure S2. (a) Raman spectra of pure DX solvents and investigated electrolytes in the region from 1050 to 1350 cm^{-1}. (b) Raman spectra of pure DX solvent, different concentrations of LiTFSI–DX, and LFSI+LiTFSI–DX electrolytes in the region from 650 to 800 cm^{-1} (S–N−S symmetric stretching mode of the FSI^- and $TFSI^-$ anions). The dotted black line and light orange solid lines represent the original spectra and the fitting results, respectively. The bands at ~720 cm^{-1} (light red line), ~730 cm^{-1} (light green line), ~743 cm^{-1} (indigo line), ~744 cm^{-1} (blue line), and ~750 cm^{-1} (light purple line) were attributed to free FSI^-, CIP (FSI^-), combining CIP ($TFSI^-$ in LBE) and AGG (FSI^- in LBE), AGG (FSI^- in LSE), and AGG ($TFSI^-$) respectively. Curve fitting was performed with Voigt (Gaussian–Lorentz) functions. The shaded region corresponds to the fitted peak profile.

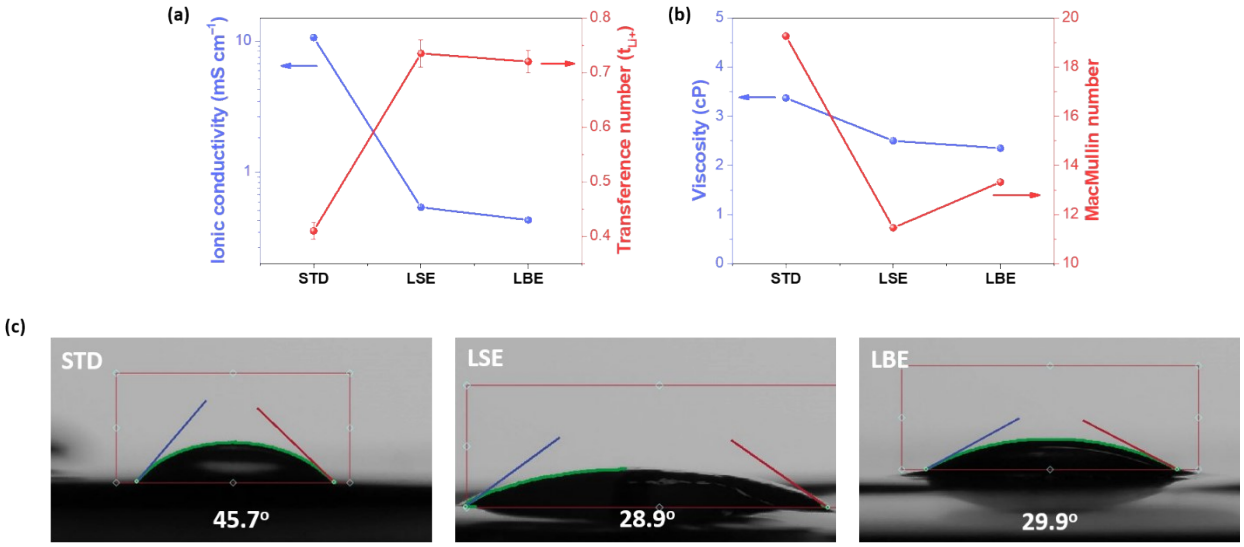

Figure S3. (a) Ionic conductivity and transference number and (b) shear viscosity and MacMullin number at 25 ℃, **(c) Contact angle snapshot of investigated electrolytes**

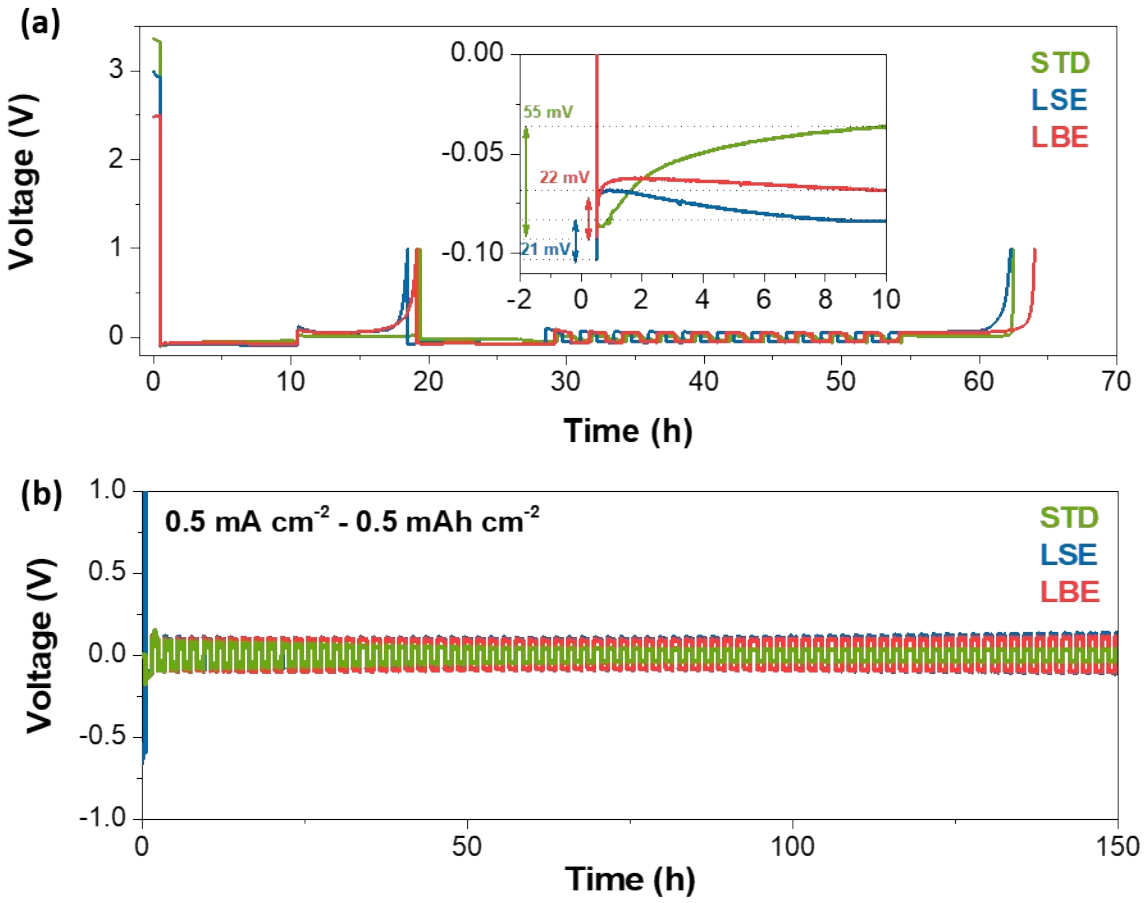

Figure S4. (a) Voltage profiles of Li||Cu cells in standard electrolyte (STD) and low concentration electrolytes (LSE and LBE). The inset shows the nucleation stage of the Li||Cu cells with investigated electrolytes. (b) Potential profiles of Li||Li symmetric cell with investigated electrolytes.

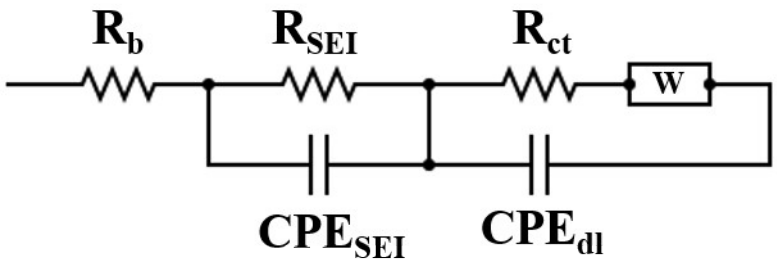

Figure S5. Electrochemical impedance spectroscopy (EIS) of the investigated electrolytes). The equivalent circuit for electrochemical impedance spectra; where R_b denotes the resistance of the bulk electrolyte; R_{SEI} and CPE_{SEI} are the resistance and the constant phase element of the SEI layer, respectively, corresponding to the semicircle at high frequency. The R_{ct} and CPE_{dl} are the resistances from charge transfer and the double-layer capacitance, respectively, which correspond to the semicircle at medium frequency. W is the Warburg element used to supplement Li^+ migration through the electrode-electrolyte interfaces and is represented by the slope line in the low-frequency region.

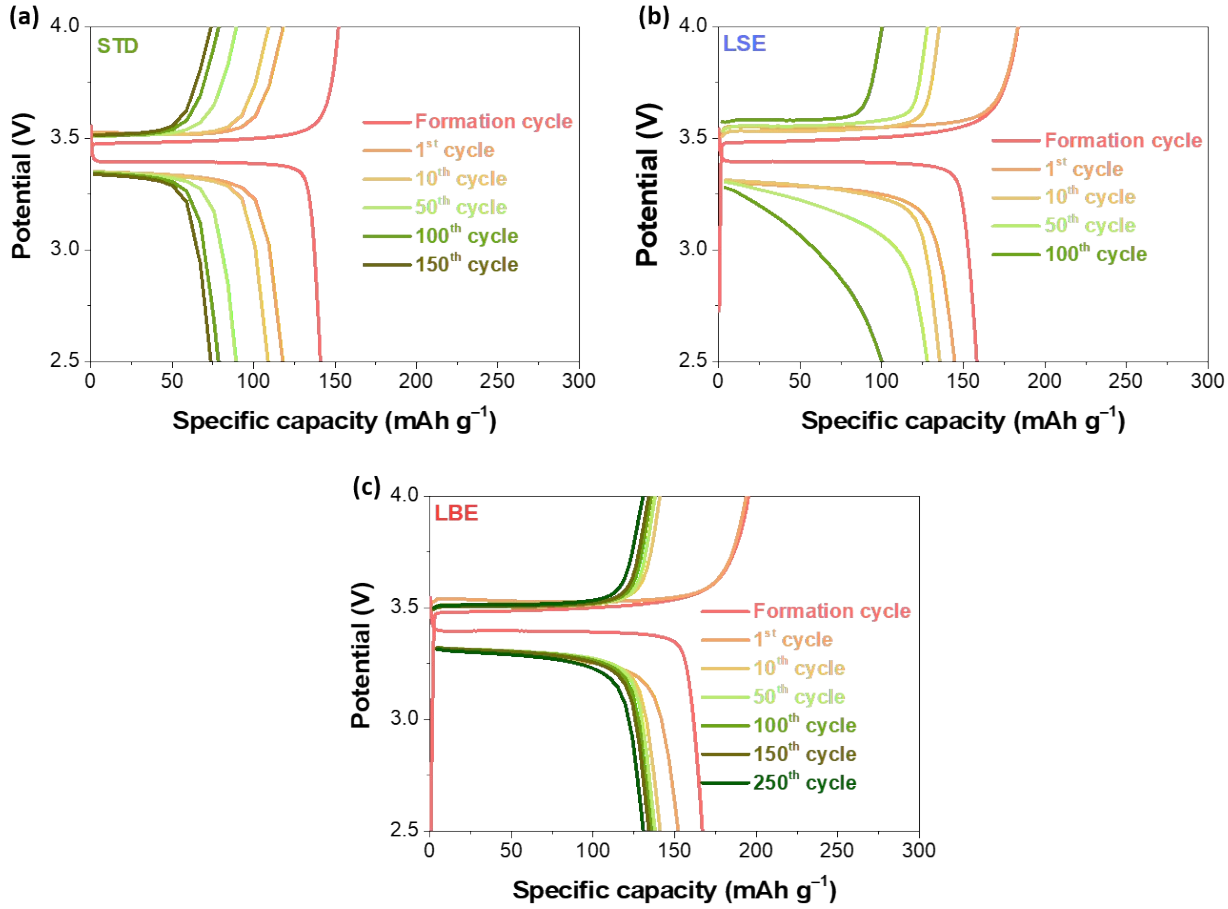

Figure S6. Voltage profiles for the Li||LFP cell cycled in (a) STD, (b) LSE, and (c) LBE at charge/discharge current densities of 0.5 C/1.0 C, respectively.

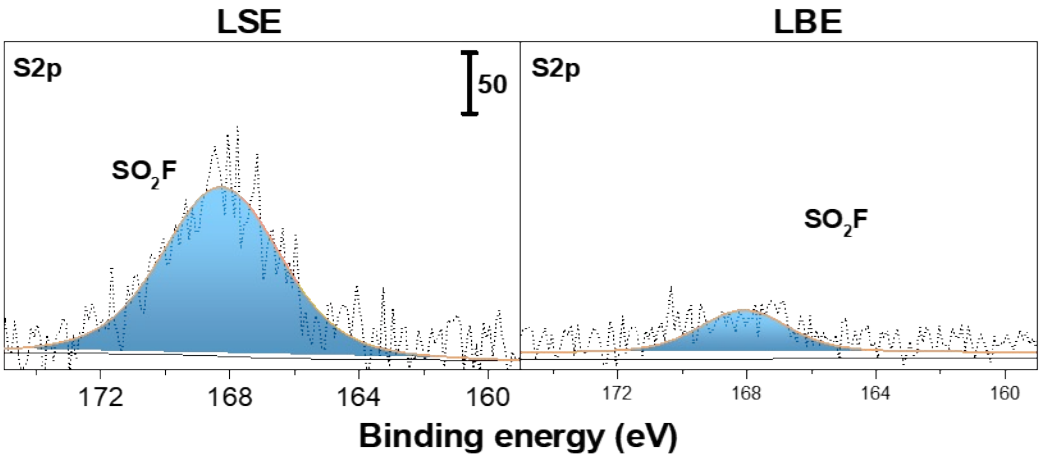

Figure S7. S 2p of XPS spectra for the SEI layers formed in investigated electrolytes.

Table S1. The total cost at different electrolytes in 1.0 liter

Electrolyte	**1.0 M $LiPF_6$ in EC:EMC:DMC (1:1:1 by volume)**	**0.5 M LiFSI - DX**	**0.3 M LiFSI + 0.2 M LiTFSI - DX**
Cost (USD/1.0L)	1,884.66	1,364.06	704.19

All costs are calculated based on Sigma-Aldrich, TCI Chemicals, or the vendors where we purchased these materials. The prices can be further decreased if large-scale products are directly purchased from chemical factories.

Table S2. Dielectric constant of various solvents

Solvent	Dielectric constant
1,4-dioxane (DX)[9]	2.2
1,2-dimethoxyethane (DME)[9]	7.3
1,2-diethoxyethane (DEE)[9]	3.9
1,3-dioxolane (DOL)[9,10]	13.0
Ethylene carbonate (EC)[9,10]	89.8
Ethyl methyl carbonate (EMC)[9,10]	2.9
Dimethyl carbonate (DMC)[11]	3.2

Table S3. Number of molecules for each of the simulation systems using classical molecular dynamics.

System	Li^+	FSI^-	$TFSI^-$	DX
LSE	40	40	-	944
LBE	40	24	16	944

Table S4. The calculated densities and ionic conductivities obtained from classical molecular dynamics, compared to experimental measurements.

Electrolyte	Density (g cm^{-3})		Ionic Conductivity (mS cm^{-1})	
	MD	**Exp.**	**MD**	**Exp.**
LSE	1.0724	1.0560	0.6429	0.5385
LBE	1.0793	1.0610	0.5622	0.4305

Table S5. Atomic ratio by XPS on surface of Li metal anode in different electrolytes collected from Li||LFP cells after 100 cycles.

Electrolyte	Atomic ratio (%)
	C (C 1s)
STD	39.02
LSE	37.48
LBE	31.84

[1] B. D. Adams, J. Zheng, X. Ren, W. Xu, J. G. Zhang, *Adv. Energy Mater.* **2018**, *8*, 1702097.

[2] Gaussian 16, Revision A.03, M. J. Frisch, G. W. Trucks, H. B. Schlegel, G. E. Scuseria, M. A. Robb, J. R. Cheeseman, G. Scalmani, V. Barone, G. A. Petersson, H. Nakatsuji, X. Li, M. Caricato, A. V. Marenich, J. Bloino, B. G. Janesko, R. Gomperts, B. Mennucci, H. P. Hratchian, J. V. Ortiz, A. F. Izmaylov, J. L. Sonnenberg, D. Williams-Young, F. Ding, F. Lipparini, F. Egidi, J. Goings, B. Peng, A. Petrone, T. Henderson, D. Ranasinghe, V. G. Zakrzewski, J. Gao, N. Rega, G. Zheng, W. Liang, M. Hada, M. Ehara, K. Toyota, R. Fukuda, J. Hasegawa, M. Ishida, T. Nakajima, Y. Honda, O. Kitao, H. Nakai, T. Vreven, K. Throssell, J. A. Montgomery Jr., J. E. Peralta, F. Ogliaro, M. J. Bearpark, J. J. Heyd, E. N. Brothers, K. N. Kudin, V. N. Staroverov, T. A. Keith, R. Kobayashi, J. Normand, K. Raghavachari, A. P. Rendell, J. C. Burant, S. S. Iyengar, J. Tomasi, M. Cossi, J. M. Millam, M. Klene, C. Adamo, R. Cammi, J. W. Ochterski, R. L. Martin, K. Morokuma, O. Farkas, J. B. Foresman, D. J. Fox, Gaussian, Inc., Wallingford CT **2016.**

[3] S. Plimpton, *J. Comput. Phys.* **1995**, *117*, 1.

[4] L. X. Dang, *J. Chem. Phys.* **1992**, *96*, 6970.

[5] J. N. Canongia Lopes, A. A. H. Pádua, *Theor. Chem. Acc.* **2012**, *131*, 1.

[6] T. A. D. D.A. Case, T.E. Cheatham, III, C.L. Simmerling, J. Wang, R.E. Duke, R., R. C. W. Luo, W. Zhang, K.M. Merz, B. Roberts, S. Hayik, A. Roitberg, G. Seabra,, A. W. G. J. Swails, I. Kolossváry, K.F. Wong, F. Paesani, J. Vanicek, R.M. Wolf, J. Liu,, S. R. B. X. Wu, T. Steinbrecher, H. Gohlke, Q. Cai, X. Ye, J. Wang, M.-J. Hsieh, G., D. R. R. Cui, D.H. Mathews, M.G. Seetin, R. Salomon-Ferrer, C. Sagui, V. Babin, T., S. G. Luchko, A. Kovalenko, and P.A. Kollman (2012), AMBER 12, University of, S. F. California.

[7] L. S. Dodda, I. C. De Vaca, J. Tirado-Rives, W. L. Jorgensen, *Nucleic Acids Res.* **2017**, *45*, W331.

[8] O. Borodin, *J. Phys. Chem. B* **2009**, *113*, 11463.

[9] D. R. Lide, *CRC Handbook of Chemistry and Physics*, **2006**.

[10] Y. X. Yao, X. Chen, C. Yan, X. Q. Zhang, W. L. Cai, J. Q. Huang, Q. Zhang, *Angew. Chemie Int. Ed.* **2020**, *60*, 4090.

[11] I. N. Daniels, Z. Wang, B. B. Laird, *J. Phys. Chem. C* **2017**, *121*, 1025.